# The 5-HT2A/1A Agonist Psilocybin Disrupts Modal Object Completion Associated with Visual Hallucinations

Michael Kometer, B. Rael Cahn, David Andel, Olivia L. Carter, and Franz X. Vollenweider

**Background:** Recent findings suggest that the serotonergic system and particularly the 5-HT2A/1A receptors are implicated in visual processing and possibly the pathophysiology of visual disturbances including hallucinations in schizophrenia and Parkinson's disease.

**Methods:** To investigate the role of 5-HT2A/1A receptors in visual processing the effect of the hallucinogenic 5-HT2A/1A agonist psilocybin (125 and 250 μg/kg vs. placebo) on the spatiotemporal dynamics of modal object completion was assessed in normal volunteers ($n = 17$) using visual evoked potential recordings in conjunction with topographic-mapping and source analysis. These effects were then considered in relation to the subjective intensity of psilocybin-induced visual hallucinations quantified by psychometric measurement.

**Results:** Psilocybin dose-dependently decreased the N170 and, in contrast, slightly enhanced the P1 component selectively over occipital electrode sites. The decrease of the N170 was most apparent during the processing of incomplete object figures. Moreover, during the time period of the N170, the overall reduction of the activation in the right extrastriate and posterior parietal areas correlated positively with the intensity of visual hallucinations.

**Conclusions:** These results suggest a central role of the 5-HT2A/1A-receptors in the modulation of visual processing. Specifically, a reduced N170 component was identified as potentially reflecting a key process of 5-HT2A/1A receptor–mediated visual hallucinations and aberrant modal object completion potential.

**Key Words:** 5-HT2A, hallucinogen, N170, P1, serotonin, visual hallucination

Despite the fact that the visual and serotonergic systems are among the most explored research topics in neuroscience, there is sparse information about the role of serotonin (5-HT) in visual processing. However, the high expression of the 5-$HT_{1A}$ (1,2) and 5-HT2A receptors (3–5) in the visual areas V1, V2, V3, and lateral suprasylvian cortex (LS) suggest a central role of the 5-$HT_{1A}$ and 2A receptors in visual processing. Furthermore, 5-HT2A receptors have been implicated in the pathogenesis of visual hallucinations in Parkinson's (6–8) and schizophrenic patients (9). In support of this view, visual hallucinations in Parkinson's patients have been associated with increased density of 5-HT2A receptors in cortical visual pathways (6,8) and effectively treated with the 5-HT2A receptor inverse agonist pimavanserin (7). Moreover, visual disturbances and hallucinations induced by the indoleamine hallucinogen psilocybin are mediated predominantly by the 5-HT2A receptor (10) and resemble, in phenomenological (11) and behavioral measurements (12), visual disturbances found in schizophrenia (13,14). Hence, there is an increasingly recognized role for the 5-HT2A receptors in the pathogenesis of visual hallucinations, but the brain mechanisms mediating between 5-HT2A receptor activation and visual hallucination are still unknown.

From the University Hospital of Psychiatry (MK, DA, FXV), Neuropsychopharmacology and Brain Imaging and Heffter Research Center, Zurich, Switzerland; Division of Geriatric Psychiatry (BRC), Department of Psychiatry, University of California, San Diego, La Jolla, California; and the Psychological Sciences (OLC), University of Melbourne, Parkville, Australia.

Address correspondence to Michael Kometer, M.Sc., University Hospital of Psychiatry, Neuropsychopharmacology and Brain Imaging and Heffter Research Center, Lenggstraße 31, CH-8032 Zurich, Switzerland; E-mail: michael.kometer@bli.uzh.ch.

Received Feb 11, 2010; revised Oct 4, 2010; accepted Oct 5, 2010.

To characterize further the role of the 5-HT2A/1A receptors in visual processing and to elucidate possible pathophysiological mechanisms of visual deficits and hallucinations, we assessed the effect of the mixed 5-HT2A/1A agonist psilocybin (125 μg/ and 250 μg/kg vs. placebo) in healthy volunteers. Electroencephalographic recordings were made while participants viewed Kanizsa and non-Kanizsa figures (Figure 1). Behavioral responses were recorded, and high-density electrical mapping with source analysis was used. This allowed for measurement of the spatiotemporal brain dynamics of visual modal object completion and its association with the appearance of visual hallucinations.

Modal object completion refers to the illusory perception of object boundaries and their enclosing surface in the absence of any direct sensory information depicting these boundaries or surfaces. The brain's ability to interpolate the existence of object surface boundaries is essential for accurate object recognition in situations in which only ambiguous or incomplete retinal information of the object is available (i.e., due to partial occlusion or poor illumination). Modal completion has been of particular interest to vision scientists because it is critical for the accurate perception of objects and the delineation of multiple objects from themselves or their background. Imaging studies provide strong evidence that the intermediate lateral occipital complex (LOC) as well as the early visual area V2 are likely to play a major role in modal completion (15–18), but the involvement of the primary visual cortex is more contentious (19). Electrophysiologic studies have revealed that modal object completion of simple figures such as Kanizsa figures is predominantly indexed by the modulation of the N170 component (20–25), which appears to be driven primarily by the two critical processes underlying modal object completion, boundary completion (22), and region-based segmentation (25). In some previous studies, the presentation of Kanizsa figures, compared with control figures, have additionally been associated with an enhancement of the earlier P1 (26) and the subsequent closure negativity ($N_{cl}$) component (22). However, because the $N_{cl}$ component is more reliably induced by more complex fragmented images and reflects successful

0006-3223/$36.00
doi:10.1016/j.biopsych.2010.10.002

recognition of complex images (27,28), it is unlikely to be as relevant to the processing of the simple Kanizsa figures used in our experiment.

The high density of 5-$HT_{1A}$ (1,2) and 5-HT2A (3–5) receptors in LOC and V2, as well as the strong activation seen in these areas after psilocybin administration during resting state (29), suggest that psilocybin might influence modal object completion. Because these processes are so critical in defining one's perceptual experience, we aimed to characterize and understand the means through which 5-HT2A/1A receptor activity can alter this fundamental aspect of visual experience.

## Methods and Materials

### Subjects

Healthy right-handed subjects (eight males, nine females, mean age 28.8 ± 3.5 years) were recruited through advertisement from the University of Zürich. All subjects were healthy according to physical examination including electrocardiography, and detailed blood analysis. The DIA-X diagnostic expert system (30) and a clinical interview was used to exclude subjects with present or antecedent psychiatric disorders, regular alcohol or substance abuse, and a history of major psychiatric disorders in first-degree relatives. The screening procedure was supplemented by the Freiburg Personality Inventory FPI (31) and Hopkins Symptom Checklist SCL-90-R (32) and a self-made substance consumption questionnaire. Because the personality trait factor "emotional lability" was identified to be a predictor for negative experiences during hallucinogen-induced altered states of consciousness (33), scores exceeding the mean value of normative FPI data by 2 SD were also used as exclusion criterion. Twelve participants reported having previous experience with psilocybin or other hallucinogens (mean lifetime experiences 5.5 ± 4.7 times). None of the subjects consumed any psychoactive substance except alcohol, nicotine, cannabis, and caffeine more than once a year.

After being informed by a written and oral description of the procedures of the study and the effects and possible risks of psilocybin administration, all volunteers gave written informed consent to participate in this study. The study was approved by the ethics committee of the University Hospital of Psychiatry, Zurich, and the use of psilocybin in humans was authorized by the Swiss Federal Office for Public Health.

### Substance and Dosing

Psilocybin was obtained through the Swiss Federal Office for Public Health. The psilocybin high-dose (HD, 250 μg/kg), low-dose (LD, 125 μg/kg), and lactose placebo (PL) were administered in gelatin capsules of identical number and appearance. On 3 experimental days, separated from each other by at least 2 weeks, the subjects came to the laboratory at 9 AM and confirmed that they had not eaten breakfast or taken caffeine that morning. In a crossover randomized design, all subjects received placebo and the two graded doses of psilocybin.

### Stimulus and Procedure

The Kanizsa experiment started 120 min postdrug ingestion. During the experiment, Kanizsa figures and control figures were presented at a distance of 1 m from the participants while they remained fixated on a central fixation-cross. All stimuli consisted of three "pacmen," each composed of a black circle with a sector of 60° removed. The removed sectors were either aligned such that the stimulus types induced the perception of an illusory triangle or they were rotated by 180° to no longer induce the illusory triangle percept ("Kanizsa" and "non-Kanizsa" conditions, respectively; see Figure 1). The stimuli subtended a visual angle of 3.7° and the support ratio, the ratio of the inducing length to the total length of one illusory contour of the triangle was 1:2. To reduce habituation, the stimuli were presented in four orientations of equal number, rotated 0°, 90°, 180°, and 270°.

Eighty-eight Kanizsa figures and 88 non-Kanizsa figures were presented with a stimulus onset asynchrony of 3 sec in a pseudorandomized order in two blocks consisting of 44 Kanizsa figures and 44 non-Kanizsa figures each. Participants were required to respond as quickly as possible with a button press according to whether they saw an illusory triangle on each trial. The response finger was counterbalanced across the subjects to control for faster reaction times of index finger compared with middle finger of the dominant hand. Stimuli remained on the monitor for 300 msec after buttonpress or for a maximum of 2000 msec.

### Psychometry

The Altered States of Consciousness (5D-ASC) rating scale (34) was used to asses the subjective effects of placebo and psilocybin with a primary focus on visual alterations and hallucinations. The 5D-ASC is a visual analogue scale consisting of 94 items that measure etiology independent alterations in consciousness, including changes in mood, perception, cognition, and experience of self and the environment. The five main factors are 1) Oceanic Boundlessness, measuring derealization and depersonalization accompanied by changes in affect ranging from heightened mood to euphoria and alterations in the sense of time; 2) Anxious Ego Dissolution, measuring ego disintegration associated with loss of self-control, thought disorder, arousal, and anxiety; 3) Visionary Restructuralization (VR) assessing visual illusions and (pseudo-)hallucinations, which includes the spectrum ranging from elementary to complex hallucinations; 4) Auditory Alterations (AA), comprising auditory illusions and (pseudo-)hallucinations; and 5) Reduction of Vigilance, assessing changes in vigilance and alertness. The results of the 5D-ASC data are given as percentage scores of maximum absolute scale values.

### Electroencephalogram Recording

Electroencephalogram (EEG) recordings were made using BioSemi (Amsterdam, The Netherlands) ActiveTwo electrode system with 64 scalp electrodes. Additional electrodes were attached on the outer canthus of each eye to record the horizontal electrooculogram (EOG) and infraorbitally and supraorbitally to the left eye to record the vertical EOG. Electrophysiologic signals were bandpass filtered at .01 to 67.0 Hz and digitized at 256 Hz.

### EEG Analysis

The EEG data were recalculated offline against average reference and bandpass filtered at 1 to 40 Hz. Correct response trials were segmented from −150 to +600 msec relative to stimulus presentation. To avoid eye movement and other artifacts in further analysis, epochs exceeding ± 100 μV in any channel were excluded. The mean ± SD number of accepted epochs per condition was 85.0 ± 5.4 for Kanizsa placebo, 85.0 ± 3.0 for non-Kanizsa placebo, 82.9 ± 4.6 for Kanizsa LD, 83.2 ± 3.7 for non-Kanizsa LD, 78.8 ± 9.4 for Kanizsa HD, 79.4 ± 9.8 for non-Kanizsa HD. These epochs were averaged time locked to Kanizsa and non-Kanizsa figure presentation time to compute the visual evoked potential (VEP). The 600-msec poststimulus period of the VEP underwent three analyses to reveal the VEP waveforms, the scalp topography, and the source localization. This combination of analysis methods has been used increasingly during the recent years because it reduces experimenter bias associated with the selection of the appropriate time window for statistical analysis of the components (35).

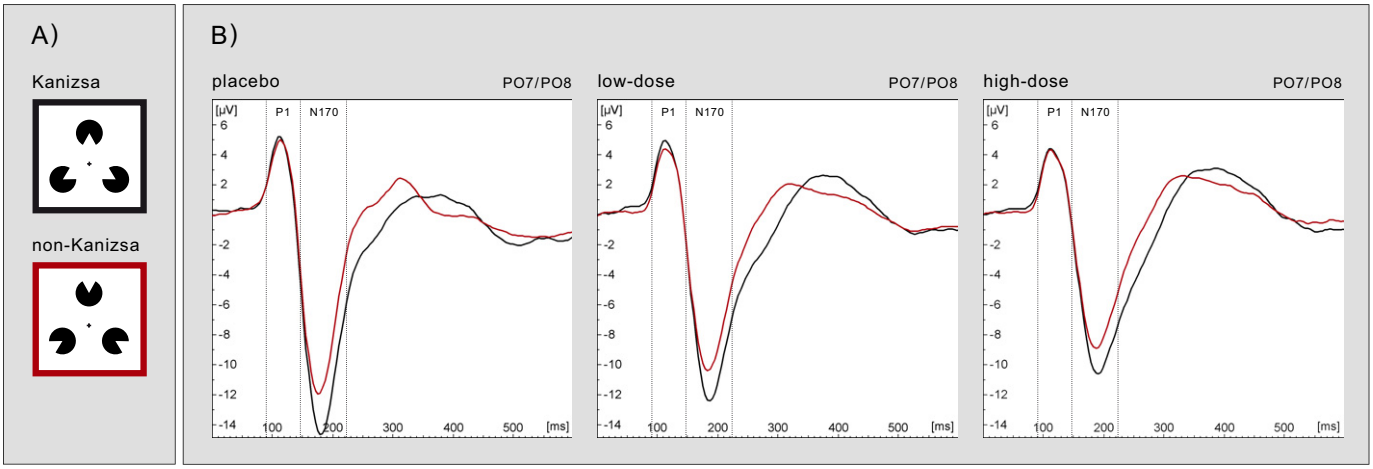


**Figure 1. (A)** Example of Kanizsa and non-Kanizsa figure. **(B)** Group-averaged visual evoked potential waveforms in response to Kanizsa figures (black traces) and non-Kanizsa figures (red traces) for placebo, low-dose, and high-dose condition averaged from the left and right posterior electrode sites PO7/PO8, where P1 and N170 amplitude was most pronounced. Dashed lines indicate the period of stable topographic configuration of the P1 and N170 component.

**Waveform Analysis.** To quantify waveform modulations, five symmetrical pairs of electrodes were selected over the maxima of the scalp topographies for the P1 and N170 components (PO7/PO8, PO3/PO4, O1/O2, P1/P2, P3/P4). The specific time windows used for calculation of the mean amplitude (vs. the baseline) were determined by the topographic analysis described next. The mean amplitudes of each of these time windows were then subjected to separate repeated-measures analysis of variance (ANOVA) with the within-subject factors dose (PL, LD, HD) electrode (PO7/PO8, PO3/PO4, O1/O2, P1/P2, P3/P4), hemiscalp (left, right), and stimulus (Kanizsa, non-Kanizsa).

**Topographic Analysis.** First, a spatial k-means cluster analysis identified the predominant topographies (also called template map) appearing in the normalized group-averaged event-related potentials (ERPs) as a function of time and experimental condition (36). This analysis was constrained by the temporal criterion that certain topographies must be observed for at least five consecutive data points (>20 msec at a 256-Hz sampling rate). The optimal number of topographies that explained the whole data set was determined by a modified cross-validation criterion (36). In a second step, we statistically verified that maps identified at the group-averaged level also appeared on the individual subject level. Therefore, at each time point, the topography of the individual subjects' ERP was compared by means of strength-independent spatial correlation to all template maps and was labeled according to the one with which it best correlated (35,37). This revealed values of relative map presence (in milliseconds), which were then subjected to a repeated-measures ANOVA using stimulus condition, map and dose as within-subject factors.

**Source Localization.** Standardized low-resolution electromagnetic tomography (sLORETA) was used to estimate the three-dimensional intracerebral current density distributions underlying the ERPs within the timeframes defined by topographic analysis. sLORETA offers a solution of the inverse problem by assuming that the smoothest of all possible activity is the most plausible (38). The solution space of sLORETA (i.e., the lead field matrix) includes 6239 voxels and was computed with a three-shell spherical head model registered to the neuroanatomic atlas of Talairach and Tournoux (Brain Imaging Centre, Montreal Neurological Institute).

*Correlational analyses* were performed to determine whether psilocybin-induced changes in the current source density within the timeframes defined by topographic analysis were related to visual or auditory hallucinations. First, the differences of the current source density between psilocybin conditions (LD and HD) and placebo were calculated separately. In a second step, these data were pooled and the Product–Moment correlations between these differences and the VR and AA scores, respectively, were calculated for each voxel. Significant correlations were identified using non-parametric permutation testing (39) that determined the critical probability threshold values for the observed *r* values with correction for multiple testing.

## Results

### Psychometrics

The subjective effects of psilocybin were assessed by the 5D-ASC rating scale. Repeated-measures ANOVA revealed a significant main effect of dose [$F(2,32) = 36.596$, $p < .00001$, $\eta^2 = .70$], factor [$F(4,64) = 12.924$, $p < .00001$, $\eta^2 = .45$], and dose × factor interaction [$F(8,128) = 7.09$, $p < .00001$, $\eta^2 = .31$]. Bonferroni-corrected post hoc analysis on the VR factor, which was of primary interest in regard to the current study, indicated a significant increase between placebo and low-dose psilocybin ($p < .00001$) as well as PL and HD psilocybin ($p < .00001$) but not LD and HD psilocybin ($p = .178$). Bonferroni-corrected post hoc analysis on the AA factor revealed a significant increase between PL and HD psilocybin ($p < .05$) but not PL and LD psilocybin ($p = 1.0$).

### Behavioral Data

Reaction time was dose-dependently increased by psilocybin [$F(2,32) = 18.841$, $p < .00001$, $\eta^2 = .54$] and was generally faster for Kanizsa compared with non-Kanizsa figures [$F(1,16) = 36.037$, $p < .0001$, $\eta^2 = .69$; Table 1]. Although psilocybin administration did lead to a dose-dependent increase in error rates [$F(2,32) = 3.3291$, $p < .05$, $\eta^2 = .17$], the error rates remained very low in all conditions (.88% for PL, 1.18% for LD, 1.92% for HD). We are therefore confident that participants were able to do the task under all drug conditions.

### Electrophysiologic Data

Under all three drug conditions both stimuli elicited prominent VEP, including the P100 and N170 component (Figure 1). The subsequent topographic analysis detected nine scalp topographies, which accounted for the 600-msec poststimulus periods across all conditions with a global explained variance of 96.74%. The first

**Table 1.** Behavioral Results Corresponding to Kanizsa and Non-Kanizsa Condition for Placebo, Low-Dose, and High-Dose Psilocybin Expressed as Mean (SD)

| | Kanizsa | Non-Kanizsa |
|---|---|---|
| Placebo | | |
| Reaction time (msec) | 514 (75) | 538 (85) |
| Error rate (%) | .88 (.93) | .88 (1.36) |
| Low-dose | | |
| Reaction time (msec) | 544 (65) | 583 (71) |
| Error rate (%) | 1.47 (1.59) | .88 (1.54) |
| High-dose | | |
| Reaction time (msec) | 592 (79) | 645 (72) |
| Error rate (%) | 1.59 (1.42) | 2.24 (3.17) |

three periods of stable scalp topographies were identical across conditions lasting from 0 to 86, 90 to 144, and 148 to 223 msec (Figure S1 in Supplement 1). These time periods were used to define the time window for quantifying the P1 and N170 VEP in a more objective manner (35) and for the subsequent source localization and correlation analysis (analysis referring to the P300 component can be found in Supplement 1).

### P1

During the time range of the P1 component (90–144 msec), a $3 \times 2 \times 5 \times 2$ repeated-measures ANOVA (using dose, hemiscalp, electrode, and stimulus as within factors) revealed a main effect only for electrode [$F(4,64) = 33.42$, $p < .00001$, $\eta^2 = .68$] and a significant interaction of electrode and dose [$F(8,128) = 3.43$, $p < .01$, $\eta^2 = .18$]. Performing Bonferroni-corrected post hoc analysis of this interaction, the P1 amplitude was found to be significantly increased from PL only at the O1/O2 electrodes by LD ($p < .05$) and HD ($p < .0001$) psilocybin. No effect of psilocybin was observed at other electrodes, nor did any other interaction reach significance. This result indicates that the effect of psilocybin on the P1 component is locally restricted to occipital electrode sites and is independent of hemiscalp and stimulus condition (Figure 2). Furthermore, the main effect for dose [$F(2,32) = .95$, $p = .39$, $\eta 2 = .06$], stimulus [$F(1,16) = .77$, $p = .39$, $\eta 2 = .05$], and hemiscalp [$F(1,16) = 1.71$, $p = .21$, $\eta 2 = .10$] did not reach significance.

To elucidate further the topographic modulation of the P1 component, the spatial correlation procedure was used first to assess the number of timeframes a given topography from the group-averaged data were present in a given condition across subjects (see Methods and Materials). These values were subjected to a repeated-measures ANOVA (using dose, stimulus, and map as within factors), which provided no evidence of topographic specificity to one stimulus or dose condition (all $ps > .15$).

Source estimation from the 90- to 144-msec period yielded activity within LOC and V2 in both hemispheres across all conditions. The psilocybin-induced increase in the P1 component over O1/O2 electrode sites seen in the VEP waveform analysis was localized most strongly in V2 and extended to LOC and V1 in the right hemisphere in the HD condition. The psilocybin induced increase in the source density did neither correlate with visual (all $ps > .17$) or auditory hallucinations (all $Ps > .98$).

### N170

To quantify the modulation of the N170 component, area measurements over the 148- to 223-msec period were subjected to a $3 \times 2 \times 5 \times 2$ repeated-measures ANOVA (using dose, hemiscalp, electrode, and stimulus as within factors). Psilocybin dose-dependently decreased the N170 amplitude [$F(2,32) = 17.170$, $p < .00001$, $\eta^2 = .52$], and Bonferroni-corrected post hoc analysis revealed that the magnitude differences were significant between all dose conditions (Figure 2). The significant interaction between dose and hemiscalp [$F(2,32) = 5.30$, $p < .05$, $\eta^2 = .25$] and the visual inspection of the VEP indicated a stronger psilocybin-induced decrease over the right compared with the left hemiscalp. In accordance with numerous previous studies (20–25), a significant main effect of the stimulus condition was observed [$F(1,16) = 35.863$, $p < .0001$, $\eta^2 = .70$], with a greater magnitude in the Kanizsa compared with the non-Kanizsa condition. This magnitude difference between Kanizsa and non-Kanizsa conditions dose-dependently decreased as re-

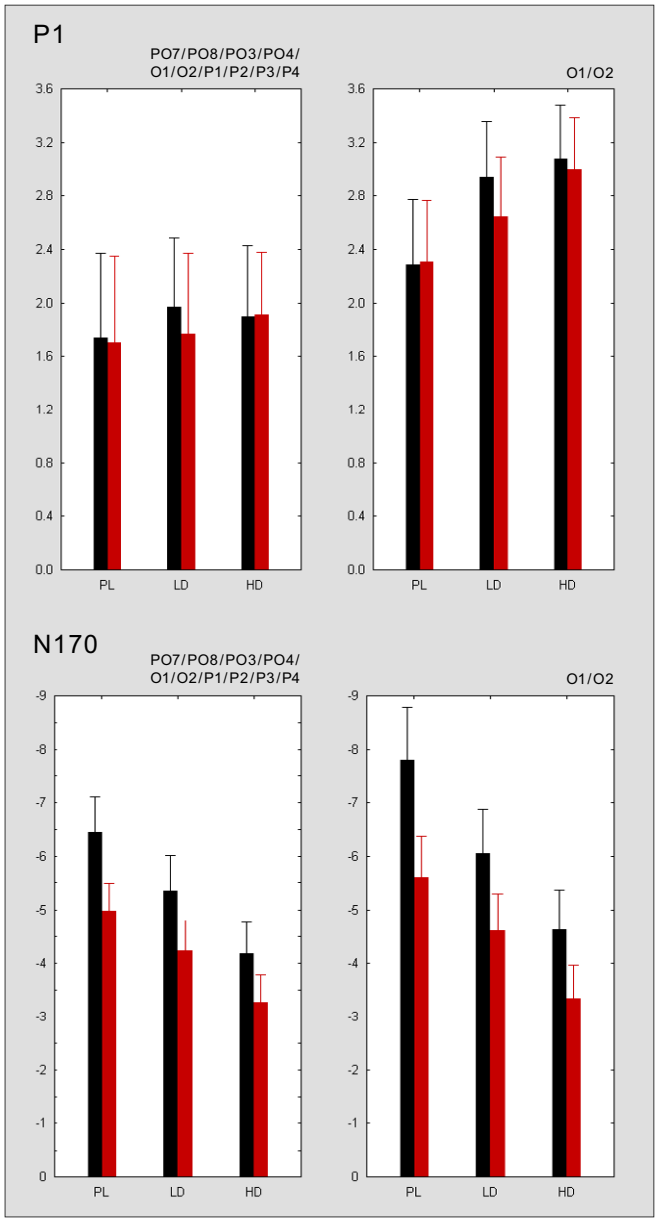


**Figure 2.** The bar graphs display mean areas of the P1 (top) and N170 (bottom) components measured from 10 parieto-occipital electrodes sites (left) and from occipital electrode sites O1/O2 (right) symmetrically localized over both hemiscalps (see Methods and Materials for details). Mean areas are displayed for Kanizsa figures (black) and non-Kanizsa figures (red) for all dose conditions (HD, high dose; LD, low dose; PL, placebo). Vertical bars denote standard deviations. The y axis presents amplitude in microvolts (μV).

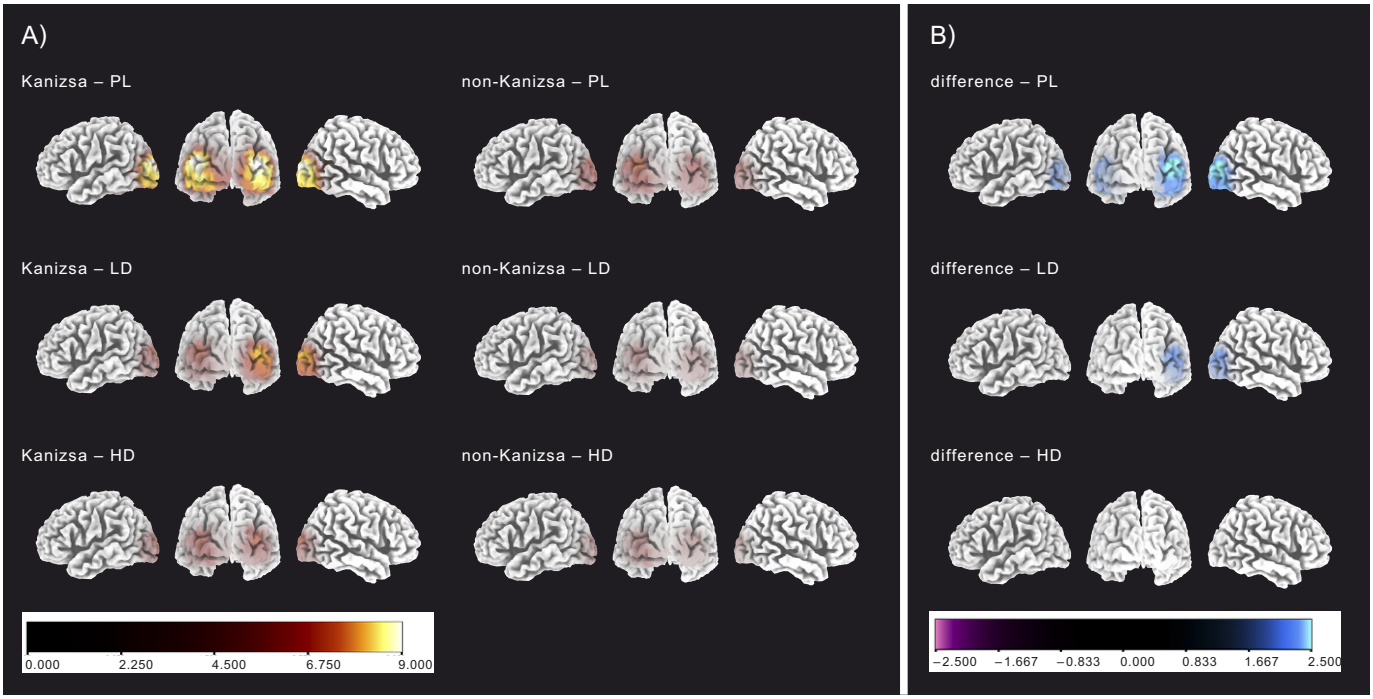


**Figure 3.** Standardized low-resolution electromagnetic tomography (sLORETA) source localization over the N170 period (148–223 msec). **(A)** Group-averaged sLORETA source estimations for each stimulus (Kanizsa, non-Kanizsa) and dose conditions over the N170 period (148–223 msec). **(B)** Group-averaged differences of the source estimations between Kanizsa and non-Kanizsa conditions. HD, high dose; LD, low dose; PL, placebo.

vealed by the significant interaction between dose and condition [$F(2,32) = 3.4485, p < .05, \eta^2 = .18$].

The topographic pattern analysis of the collective data indicated that the effects of strength modulation in the electrical field were not associated with topographic modulations. This was subsequently confirmed by subjecting individual subject data to repeated-measures ANOVA (all $ps > .25$).

The source estimation revealed activity within LOC and V2 in both hemispheres in all conditions (Figure 3). Current source density was stronger within right-lateralized LOC and V2 in the Kanizsa compared with non-Kanizsa condition. Psilocybin dose-dependently decreased the differential activation of the two stimulus conditions and reduced the current source density within LOC, V2, and fusiform gyrus in both stimulus conditions. The psilocybin-induced current source-density reduction over right-lateralized LOC, V2, and posterior parietal areas correlated significantly with the increased intensity of visual hallucinations (Figure 4), whereas no correlation could be revealed with auditory hallucinations (all $ps > .64$).

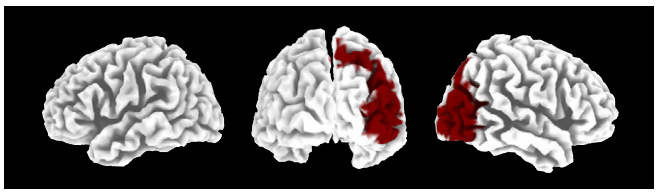

**Figure 4.** Correlation analysis over the N170 period (148–223 msec). The voxelwise correlation between visual hallucinations and placebo—psilocybin current source-density difference revealed that psilocybin-induced decrease in current source density in right extrastriate areas and posterior parietal areas over the N170 period (148–223 msec) positively correlated with the intensity of visual hallucinations (significant areas $p < .05$ are shown in red). One hundred ninety-four voxels reached .05 significance criterion with a mean $r$ value of .57.

## Discussion

This investigation revealed three main findings. First, the data indicate that the mixed 5-HT2A/1A-receptor agonist psilocybin distinctively modulates the two early visual processing components. Specifically, whereas we found a strong dose-dependent decrease of the N170 component (148- to 223-msec poststimulus), the earlier visual P1 component (90- to 144-msec poststimulus) was slightly increased over occipital electrode sites. Second, the reduction of the N170 component was stronger for the Kanizsa figure condition compared with the non-Kanizsa condition. Third, during this time range the decrease in activation over right-lateralized extrastriate and posterior parietal cortex correlated with the reported intensity of visual hallucinations.

The timeframe of the N170 component has been regarded as a critical period for object completion on the basis of numerous findings of enhanced N170 amplitude and underlying LOC and V2 activation evoked by Kanizsa compared with control figures (20–25). The preferential reduction of the N170 amplitude in Kanizsa compared with non-Kanizsa condition by psilocybin indicates a central role of the 5-HT2A/1A receptors in object completion. Because two subprocesses of object completion, boundary completion (22) and region-based segmentation (25), have been shown to underlay the enhanced N170 amplitude in the Kanizsa condition, it would be interesting to investigate further which of these two subprocesses is modulated by signal transmission at 5-HT2A/1A receptors.

The finding that psilocybin slightly enhanced P1 amplitude may reflect a generalized effect of 5-HT2A/1A mediated increase in perceived brightness, which is often reported after indolamine hallucinogen administration (40). This is supported by previous studies using comparable Kanizsa figures showing the P1 component to be sensitive to stimulus brightness (41) as well as eccentricity (20) and symmetry (41).

Given that psilocybin strongly decreased the N170 amplitude in both the Kanizsa and the non-Kanizsa conditions, we suggest that it modulates additional processes beyond proper object completion. Disruption of these processes might play a role in visual hallucinations because their reported intensity was significantly correlated with the three-dimensional current source-density reduction over right-lateralized LOC, V2, and posterior parietal areas during the timeframe of the N170 component. This localization agrees with previous imaging studies reporting decreased extrastriate activation in response to external visual stimuli in patients with visual hallucinations compared with patients without hallucinations (42–44). Furthermore, we found decreased activation specifically during the time range of the N170 component. Decreased activation during this time range has been previously reported in studies investigating acoustic (45,46) and visual hallucinations (23). We therefore suggest that decreased stimulus-induced activation in modality-specific cortical areas during the time range of the N1/N170 component may be a characteristic of acoustic as well as visual hallucinations. This relationship between the increased intensity of visual hallucinations and the decreased stimulus-evoked activation of extrastriate areas during the time range of the N170 component could reflect a competition for neuronal resources in the processing of internally (hallucination) and externally generated (sensory-driven) information (46,47). A comparable mechanism has previously been suggested to be relevant in the formation of acoustic hallucinations (48). Increased extrastriate activation, which could interfere with the processing of external stimuli, has been observed previously during visual hallucinations in the absence of external stimulation in various psychiatric disorders (43,49–51) as well as after psilocybin administration (29). In line with this interpretation, we additionally found a correlation between reduced posterior parietal activation and hallucinatory severity. The posterior parietal cortex controls attention to visual stimuli by modulating visual cortex activity (52) during the time range of the N170 component (53). The reduced posterior parietal activation might therefore reflect a psilocybin-induced failure to allocate attention and thus neuronal resources to external stimuli.

Importantly, we identified reduced extrastriate visual cortex activation during the time range of the N170 as a potential key component of 5-HT2A/1A agonist-induced visual hallucinations. Such a mechanism could also underlie the visual disturbances and hallucinations reported in Parkinson and schizophrenia patients, because increased 5-HT2A receptor densities have been found in these conditions and associated with visual hallucinations (6,8,9). In support of this notion, Parkinson's patients with visual hallucinations showed more pronounced impairments in visual object recognition (54,55) and more prominent reductions in extrastriate cortex activation to visual stimuli than patients without hallucinations (44). Moreover, a reduction of the N170 component has also been reported in schizophrenia patients and associated with visual hallucinations using Kanizsa figures (23). These observations are in line with our finding of a correlation between reduced extrastriate activation during the time range of the N170 component and the intensity of visual hallucinations. It is noteworthy, however, that two other previous studies using Kanizsa figures in schizophrenia reported either no reduction (24) or a reduction only at a trend level (56). The apparent discrepancy between these results and our findings may result from the fact that only about 30% of schizophrenia patients typically report visual hallucinations (57) and many of the patients tested were medicated with atypical antipsychotics with 5-HT2A antagonistic activity. It might therefore be possible that a disrupted 5-HT2A receptor system may be relevant only to a subgroup of schizophrenia patients. We did not find a decrease of the P1 component after psilocybin administration, and the robust reduction of the P1 component reported in schizophrenia (23,24,56,58) was not associated with psychotic symptoms (58); these findings suggest that the reduction of the P1 component in schizophrenia is not related to serotonergic alterations and may represent an endophenotype of the schizophrenia spectrum (58,59).

Because psilocybin is a mixed 5-HT2A/1A agonist (60) resulting in downstream effects on the dopamine systems (61), the exact pharmacologic mechanisms of the observed psilocybin effects require further investigation. However, converging lines of evidence indicate that psilocybin's psychotomimetic effects are mediated through the 5-HT2A-receptor activation (10,62). For example, behavioral effects of psilocybin are lacking in 5-HT2A receptor knockout mice (63), and in humans, nearly all psychotomimetic effects including visual distortions and hallucinations can be blocked by the 5-HT2A antagonist ketanserin (64,65) but not by blocking downstream dopaminergic effects with haloperidol (64). These findings, in combination with evidence regarding the importance of the 5-HT2A receptors in the pathophysiology of visual hallucinations (6–9), indicate that the reported effects of psilocybin are likely to be mediated by 5-HT2A receptor activation. However, given that 5-$HT_{1A}$ receptors additionally influence the psychotomimetic effects of indolamine hallucinogens (66) and 5-$HT_{1A}$ receptors are widespread in the visual cortex (1,2), further studies are needed to exclude an additional contribution of 5-$HT_{1A}$ receptor on the spatiotemporal dynamics of visual object completion and hallucinations.

*This work was supported by the Swiss Neuromatrix Foundation, Switzerland (MK, FXV) and the Heffter Research Institute, Santa Fe, New Mexico (RC, DA). We thank R.D. Pascual-Marqui for his technical support and for the development of LORETA software package. All authors report no biomedical financial interests or potential conflicts of interest with respect to this study.*

*Supplementary material cited in this article is available online.*

1. Dyck RH, Cynader MS (1993): Autoradiographic localization of serotonin receptor subtypes in cat visual cortex: Transient regional, laminar, and columnar distributions during postnatal development. *J Neurosci* 13: 4316–4338.
2. Gerstl F, Windischberger C, Mitterhauser M, Wadsak W, Holik A, Kletter K, *et al.* (2008): Multimodal imaging of human early visual cortex by combining functional and molecular measurements with fMRI and PET. *Neuroimage* 41:204–211.
3. Jakab RL, Goldman-Rakic PS (1998): 5-hydroxytryptamine 2A serotonin receptors in the primate cerebral cortex: possible site of action of hallucinogenic and antipsychotic drugs in pyramidal cell apical dendrites. *Proc Natl Acad Sci USA* 95:735–740.
4. Adams KH, Pinborg LH, Svarer C, Hasselbalch SG, Holm S, Haugbol S, *et al.* (2004): A database of (18F)-altanserin binding to 5-HT2A receptors in normal volunteers: Normative data and relationship to physiological and demographic variables. *Neuroimage* 21:1105–1113.
5. Watakabe A, Komatsu Y, Sadakane O, Shimegi S, Takahata T, Higo N, *et al.* (2009): Enriched expression of serotonin 1B and 2A receptor genes in macaque visual cortex and their bidirectional modulatory effects on neuronal responses. *Cereb Cortex* 19:1915–1928.
6. Ballanger B, Strafella AP, van ET, Zurowski M, Rusjan PM, Houle S, *et al.* (2010): Serotonin 2A receptors and visual hallucinations in Parkinson disease. *Arch Neurol* 67:416–421.
7. Meltzer HY, Mills R, Revell S, Williams H, Johnson A, Bahr D, *et al.* (2010): Pimavanserin, a serotonin (2A) receptor inverse agonist, for the treatment of Parkinson's disease psychosis. *Neuropsychopharmacology* 35: 881–892.
8. Huot P, Johnston TH, Darr T, Hazrati LN, Visanji NP, Pires D, *et al.* (2010): Increased 5-HT2A receptors in the temporal cortex of parkinsonian patients with visual hallucinations. *Mov Disord* 25:1399–1408.

9. Gonzalez-Maeso J, Ang RL, Yuen T, Chan P, Weisstaub NV, Lopez-Gimenez JF, *et al.* (2008): Identification of a serotonin/glutamate receptor complex implicated in psychosis. *Nature* 452:93–97.
10. Geyer MA, Vollenweider FX (2008): Serotonin research: Contributions to understanding psychoses. *Trends Pharmacol Sci* 29:445–453.
11. Vollenweider FX, Geyer MA (2001): A systems model of altered consciousness: integrating natural and drug-induced psychoses. *Brain Res Bull* 56:495–507.
12. Carter OL, Pettigrew JD, Burr DC, Alais D, Hasler F, Vollenweider FX (2004): Psilocybin impairs high-level but not low-level motion perception. *Neuroreport* 15:1947–1951.
13. Chen Y, Levy DL, Sheremata S, Holzman PS (2004): Compromised late-stage motion processing in schizophrenia. *Biol Psychiatry* 55:834–841.
14. Chen Y, Nakayama K, Levy D, Matthysse S, Holzman P (2003): Processing of global, but not local, motion direction is deficient in schizophrenia. *Schizophr Res* 61:215–227.
15. Mendola JD, Dale AM, Fischl B, Liu AK, Tootell RB (1999): The representation of illusory and real contours in human cortical visual areas revealed by functional magnetic resonance imaging. *J Neurosci* 19:8560–8572.
16. Halgren E, Mendola J, Chong CD, Dale AM (2003): Cortical activation to illusory shapes as measured with magnetoencephalography. *Neuroimage* 18:1001–1009.
17. Stanley DA, Rubin N (2003): fMRI activation in response to illusory contours and salient regions in the human lateral occipital complex. *Neuron* 37:323–331.
18. Montaser-Kouhsari L, Landy MS, Heeger DJ, Larsson J (2007): Orientation-selective adaptation to illusory contours in human visual cortex. *J Neurosci* 27:2186–2195.
19. Seghier ML, Vuilleumier P (2006): Functional neuroimaging findings on the human perception of illusory contours. *Neurosci Biobehav Rev* 30: 595–612.
20. Murray MM, Wylie GR, Higgins BA, Javitt DC, Schroeder CE, Foxe JJ (2002): The spatiotemporal dynamics of illusory contour processing: Combined high-density electrical mapping, source analysis, and functional magnetic resonance imaging. *J Neurosci* 22:5055–5073.
21. Murray MM, Foxe DM, Javitt DC, Foxe JJ (2004): Setting boundaries: brain dynamics of modal and amodal illusory shape completion in humans. *J Neurosci* 24:6898–6903.
22. Murray MM, Imber ML, Javitt DC, Foxe JJ (2006): Boundary completion is automatic and dissociable from shape discrimination. *J Neurosci* 26: 12043–12054.
23. Spencer KM, Nestor PG, Perlmutter R, Niznikiewicz MA, Klump MC, Frumin M, *et al.* (2004): Neural synchrony indexes disordered perception and cognition in schizophrenia. *Proc Natl Acad Sci U S A* 101:17288–17293.
24. Foxe JJ, Murray MM, Javitt DC (2005): Filling-in in schizophrenia: A high-density electrical mapping and source-analysis investigation of illusory contour processing. *Cereb Cortex* 15:1914–1927.
25. Yoshino A, Kawamoto M, Yoshida T, Kobayashi N, Shigemura J, Takahashi Y, *et al.* (2006): Activation time course of responses to illusory contours and salient region: A high-density electrical mapping comparison. *Brain Res* 1071:137–144.
26. Brodeur M, Lepore F, Lepage M, Bacon BA, Jemel B, Debruille JB (2008): Alternative mode of presentation of Kanizsa figures sheds new light on the chronometry of the mechanisms underlying the perception of illusory figures. *Neuropsychologia* 46:554–566.
27. Doniger GM, Foxe JJ, Murray MM, Higgins BA, Snodgrass JG, Schroeder CE, *et al.* (2000): Activation timecourse of ventral visual stream object-recognition areas: high density electrical mapping of perceptual closure processes. *J Cogn Neurosci* 12:615–621.
28. Sehatpour P, Dias EC, Butler PD, Revheim N, Guilfoyle DN, Foxe JJ, *et al.* (2010): Impaired visual object processing across an occipital-frontal-hippocampal brain network in schizophrenia: An integrated neuroimaging study. *Arch Gen Psychiatry* 67:772–782.
29. Vollenweider FX, Leenders KL, Scharfetter C, Maguire P, Stadelmann O, Angst J (1997): Positron emission tomography and fluorodeoxyglucose studies of metabolic hyperfrontality and psychopathology in the psilocybin model of psychosis. *Neuropsychopharmacology* 16:357–372.
30. Wittchen HU, Pfister H (1997): *DIA-X-interview*. Frankfurt: Swets Test Services.
31. Fahrenberg J, Hampel R, Selg H (1984): *Das Freiburger Persönlichkeitsinventar FPI, 4th ed*. Göttingen: Hogrefe.
32. Derogatis LR (1994): SCL-90-R *Symposiumtom Checklist-90-R. Administration, scoring and procedures manual, 3rd ed.* Minneapolis, MN: National Computer Systems.
33. Dittrich A (1994): Psychological aspects of altered states of consciousness of the LSD type: Measurements of their basic dimensions and prediction of individual differences. In: Pletscher A, Ladewig D, editors. *50 Years of LSD. Current Status and Perspectives of Hallucinogens*. New York: Parthenon, pp 101–118.
34. Dittrich A (1998): The standardized psychometric assessment of altered states of consciousness (ASCs) in humans. *Pharmacopsychiatry* 31:80–84.
35. Murray MM, Brunet D, Michel CM (2008): Topographic ERP analyses: A step-by-step tutorial review. *Brain Topogr* 20:249–264.
36. Pascual-Marqui RD, Michel CM, Lehmann D (1995): Segmentation of brain electrical activity into microstates: Model estimation and validation. *IEEE Trans Biomed Eng* 42:658–665.
37. Brandeis D, Lehmann D, Michel CM, Mingrone W (1995): Mapping event-related brain potential microstates to sentence endings. *Brain Topogr* 8:145–159.
38. Pascual-Marqui RD (2002): Standardized low-resolution brain electromagnetic tomography (sLORETA): Technical details. *Methods Find Exp Clin Pharmacol* 24(suppl D):5–12.
39. Nichols TE, Holmes AP (2002): Nonparametric permutation tests for functional neuroimaging: A primer with examples. *Hum Brain Mapp* 15:1–25.
40. Siegel RK, Jarvik ME (1975): Drug-induced hallucinations in animals and man. In: Siegel RK, West LJ, editors *Hallucinations. Behavior, Experience and Theory*. New York: Wiley, 81–161.
41. Proverbio AM, Zani A (2002): Electrophysiological indexes of illusory contours perception in humans. *Neuropsychologia* 40:479–491.
42. Howard R, Williams S, Bullmore E, Brammer M, Mellers J, Woodruff P, *et al.* (1995): Cortical response to exogenous visual stimulation during visual hallucinations. *Lancet* 345:70.
43. Ffytche DH, Howard RJ, Brammer MJ, David A, Woodruff P, Williams S (1998): The anatomy of conscious vision: An fMRI study of visual hallucinations. *Nat Neurosci* 1:738–742.
44. Meppelink AM, de Jong BM, Renken R, Leenders KL, Cornelissen FW, van LT (2009): Impaired visual processing preceding image recognition in Parkinson's disease patients with visual hallucinations. *Brain* 132:2980–2993.
45. Tiihonen J, Hari R, Naukkarinen H, Rimon R, Jousmäki V, Kajola M (1992): Modified activity of the human auditory cortex during auditory hallucinations. *Am J Psychiatry* 149:255–257.
46. Hubl D, Koenig T, Strik WK, Garcia LM, Dierks T (2007): Competition for neuronal resources: How hallucinations make themselves heard. *Br J Psychiatry* 190:57–62.
47. Allen P, Laroi F, McGuire PK, Aleman A (2008): The hallucinating brain: a review of structural and functional neuroimaging studies of hallucinations. *Neurosci Biobehav Rev* 32:175–191.
48. Ford JM, Roach BJ, Jorgensen KW, Turner JA, Brown GG, Notestine R, *et al.* (2009): Tuning in to the voices: A multisite FMRI study of auditory hallucinations. *Schizophr Bull* 35:58–66.
49. Silbersweig DA, Stern E, Frith GH, Cahill C, Holmes A, Grootoonk S, *et al.* (1995): A functional neuroanatomy of hallucinations in schizophrenia. *Nature* 378:176–179.
50. Holroyd S, Wooten GF (2006): Preliminary FMRI evidence of visual system dysfunction in Parkinson's disease patients with visual hallucinations. *J Neuropsychiatry Clin Neurosci* 18:402–404.
51. Oertel V, Rotarska-Jagiela A: Van dV. V, Haenschel C, Maurer K, Linden DE (2007): Visual hallucinations in schizophrenia investigated with functional magnetic resonance imaging. *Psychiatry Res* 156: 269–273.
52. Bressler SL, Tang W, Sylvester CM, Shulman GL, Corbetta M (2008): Top-down control of human visual cortex by frontal and parietal cortex in anticipatory visual spatial attention. *J Neurosci* 28: 10056–10061.
53. Rose M, Schmid C, Winzen A, Sommer T, Buchel C (2005): The functional and temporal characteristics of top-down modulation in visual selection. *Cereb Cortex* 15:1290–1298.
54. Meppelink AM, Koerts J, Borg M, Leenders KL, van Laar T (2008): Visual object recognition and attention in Parkinson's disease patients with visual hallucinations. *Mov Disord* 23:1906–1912.
55. Koerts J, Borg MA, Meppelink AM, Leenders KL, van BM, van LT (2010): Attentional and perceptual impairments in Parkinson's disease with visual hallucinations. *Parkinsonism Relat Disord* 16:270–274.

56. Spencer KM, Nestor PG, Niznikiewicz MA, Salisbury DF, Shenton ME, McCarley RW (2003): Abnormal neural synchrony in schizophrenia. *J Neurosci* 23:7407–7411.
57. Bracha HS, Wolkowitz OM, Lohr JB, Karson CN, Bigelow LB (1989): High prevalence of visual hallucinations in research subjects with chronic schizophrenia. *Am J Psychiatry* 146:526–528.
58. Yeap S, Kelly SP, Sehatpour P, Magno E, Garavan H, Thakore JH, *et al.* (2008): Visual sensory processing deficits in schizophrenia and their relationship to disease state. *Eur Arch Psychiatry Clin Neurosci* 258:305–316.
59. Yeap S, Kelly SP, Sehatpour P, Magno E, Javitt DC, Garavan H, *et al.* (2006): Early visual sensory deficits as endophenotypes for schizophrenia: High-density electrical mapping in clinically unaffected first-degree relatives. *Arch Gen Psychiatry* 63:1180–1188.
60. McKenna DJ, Repke DB, Peroutka SJ (1990): Differential interactions of indolealkylamines with 5-hydroxytrypamine receptor subtypes. *Neuropharmacology* 29:193–198.
61. Vollenweider FX, Vontobel P, Hell D, Leenders KL (1998): 5-HT modulation of dopamine release in basal ganglia in psilocybin-induced psychosis in man—a PET study with [11C] raclopride. *Neuropsychopharmacology* 20:424–433.
62. Gonzalez-Maeso J, Sealfon SC (2009): Psychedelics and schizophrenia. *Trends Neurosci* 32:225–232.
63. Gonzalez-Maeso J, Weisstaub NV, Zhou M, Chan P, Ivic L, Ang R, *et al.* (2007): Hallucinogens recruit specific cortical 5-HT(2A) receptor-mediated signaling pathways to affect behavior. *Neuron* 53:439–452.
64. Vollenweider FX, Vollenweider-Scherpenhuyzen MFI, Bäbler A, Vogel H, Hell D (1998): Psilocybin induces schizophrenia-like psychosis in humans via a serotonin-2 agonist action. *Neuroreport* 9:3897–3902.
65. Carter OL, Burr DC, Pettigrew JD, Wallis GM, Hasler F, Vollenweider FX (2005): Using psilocybin to investigate the relationship between attention, working memory, and the serotonin 1A and 2A receptors. *J Cogn Neurosci* 17:1497–1508.
66. Nichols DE (2004): Hallucinogens. *Pharmacol Ther* 101:131–181.